Flow Reconstruction with Neural Network-based Reduced Order Modeling

Allan Moreira de Carvalho
email allan.carvalho@ufabc.edu.br

Federal University of ABC - Santo André, Brazil
April 27, 2023

Abstract

The performance of rocket engines relies heavily on the flow of gases through the nozzle. Therefore, a thorough understanding of flow and heat transfer in rocket nozzles is essential for their design and optimization. In this paper, we propose a methodology that utilizes neural networks and singular value decomposition to reconstruct the internal flow and heat transfer fields in a rocket nozzle. The methodology involves two main steps. Firstly, we use both low and high fidelity computational fluid dynamics (CFD) analyses to simulate the flow of gases through the nozzle and predict the heat transfer. Secondly, we decompose the data matrix generated from the CFD simulations using singular value decomposition (SVD) and train a neural network to learn the relationship between the dominant modes obtained from the SVD of both fidelity simulations.The trained neural network can then be used to reconstruct the flow and heat transfer fields from the low fidelity solutions. The proposed methodology has been shown to accurately predict fluid flows and, to some extent, temperature and heat flux in the nozzle walls. The surrogate model developed using this methodology has great potential for improving the design and optimization of nozzle flows.

1 Introduction

In the field of rocket propulsion, accurate prediction of heat transfer in nozzle flow plays a critical role in designing and optimizing rocket engines (ZHANG, 2011). However, existing methods for predicting heat transfer often suffer from high computational complexity, making them impractical for engineering design purposes. To address this challenge, we propose a flow reconstruction (LUI; WOLF, 2019; YU; HESTHAVEN, 2019) technique that combines order reduction using Singular Value Decomposition (SVD)(GOLUB; VAN LOAN, 2013) with neural network modeling (BRUNTON; KUTZ, 2019). While the individual techniques are not novel, our approach offers a combination of these methods for accurate and efficient prediction of internal flow and thermal fields in the nozzle, leading to highly accurate fluid flow predictions. Furthermore, the use of neural network modeling enhances the accuracy of our approach by capturing the complex nonlinearities of the flow. Overall, our flow reconstruction technique has the potential to significantly improve the design and optimization of conjugate heat transfer CFD problems, providing valuable insights into the underlying physical phenomena while reducing computational complexity.

2 Methodology

Flow reconstruction (YU; HESTHAVEN, 2019) is a technique used to recover high-fidelity computational fluid dynamics (CFD) simulations from low-fidelity ones. This can be accomplished using neural networks and singular value decomposition (SVD). The proposed methodology is data-driven and consists of three main steps.

In the first step, the data is generated. To generate a set of high fidelity simulations, the input parameters are varied to cover a wide range of flow conditions. To generate a set of low fidelity simu-

lations, the resolution is reduced, the model is simplified, or a less accurate numerical method is used. In the second step, both sets of simulations are reduced to a set of basis functions coefficients using SVD, which capture the dominant modes of variation in the flow fields. This allows for a more efficient representation of the flow field and facilitates the use of neural networks for flow reconstruction.

The final step of the proposed flow reconstruction technique involves training a neural network to map the low-fidelity reduced simulations to their corresponding high-fidelity counterparts. During the online training stage, the neural network takes a set of low-fidelity basis coefficients as input and generates a set of coefficients for the high-fidelity reduced basis as output. Once trained, the neural network can be used for inference in the offline stage. During inference, the low-fidelity simulation in full space is projected onto the basis coefficients using SVD. These coefficients are then used as input to the trained neural network to predict the corresponding high-fidelity basis coefficients. Finally, a reverse projection operation is performed on the predicted coefficients to recover the high-fidelity simulation in full space. Figure provides a schematic representation of this reconstruction approach.

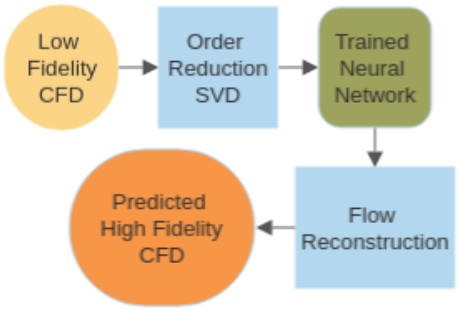

Figure 1: Flow reconstruction inference flow chart.

2.1 Step 1: Data Generation using CFD Analysis

In this work, we aim to develop a surrogate model that predicts the 2D viscous airflow, temperature, and heat flux on the inner surface of a nozzle, using only quasi-1D simulations. For the model to be useful for design purposes, it must also be sensitive to geometrical parameters. Therefore, we focus on two key design variables: the thickness of the nozzle wall (t_w) and the shape of the nozzle wall, which is defined by the y-coordinate of a Bezier control point ($CP3_y$), as shown in Figure 2.

To begin, we use Latin Hypercube sampling (LHS) (MCKAY; BECKMAN; CONOVER, 1979) to sample 30 design variables in the range provided in Table 1, as shown in Figure 3. We consider a set of N pairs of design variables denoted as $\Xi^i = \{t_w, CP3_y\}^i$. For each pair, we collect a low-fidelity snapshot ($\mathbf{L}^i \in \mathbb{R}^{S_L}$) and a high-fidelity snapshot ($\mathbf{H}^i \in \mathbb{R}^{S_H}$) that contain the modeled variables.

To store the low-fidelity and high-fidelity snapshots, we use two matrices, denoted by $\mathbf{A}_L$ and $\mathbf{A}_H$, respectively. The low-fidelity snapshots are stored in $\mathbf{A}_L$ according to Equation (1), while the high-fidelity snapshots are stored in $\mathbf{A}_H$ according to Equation (2).

$$\mathbf{A}_L = \left[\mathbf{L}^1 | \dots | \mathbf{L}^N\right]^{S_L \times N} \tag{1}$$

$$\mathbf{A}_H = \left[\mathbf{H}^1 | \dots | \mathbf{H}^N\right]^{S_H \times N} \tag{2}$$

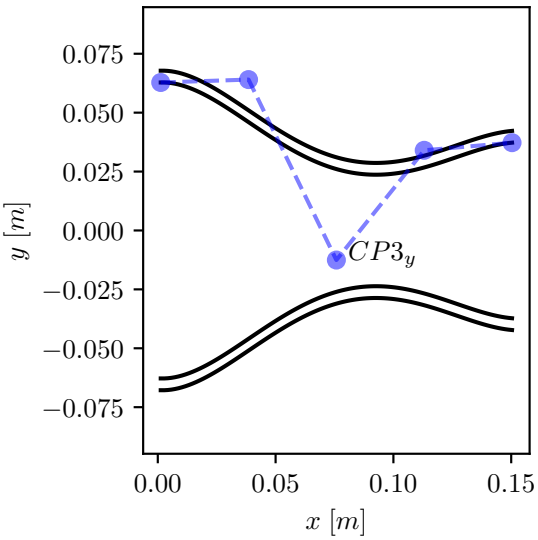

Figure 2: Nozzle shape defined by the thickness of the wall (t_w) and the y-coordinate of a Bezier control point ($CP3_y$).

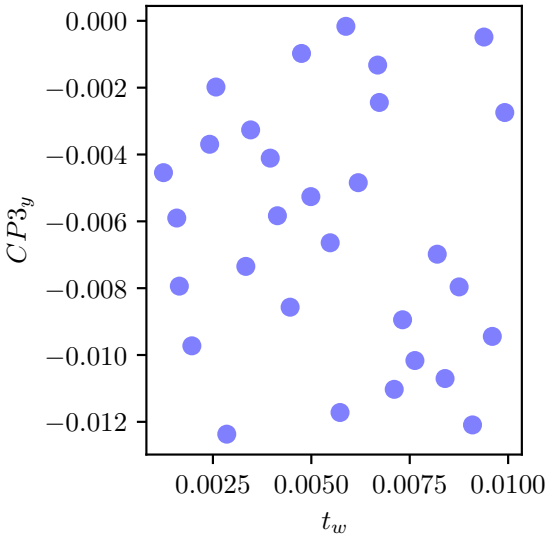

Figure 3: Latin Hypercube Sampling of 30 design variables within the sampling ranges given in Table 1.

	Minimum	Maximum
t_w	0.0010 m	0.0100 m
$CP3_y$	-0.0125 m	0.0000 m

Table 1: Sampling ranges for the design variables.

2.1.1 Low fidelity model

The low-fidelity model used in this study is an in-house finite volume solver based on the quasi-1D Euler equations (HIRSCH, 2007). These equations simplify the full problem by neglecting viscous and heat transfer effects but account for compressibility effects, which reduces computational costs while still capturing the important behavior of transonic and supersonic flows. The boundary conditions at the inlet include total pressure ($p_0 = 800$ kPa) and total temperature ($T_0 = 600$ K), while the outlet boundary condition is static pressure ($p_b = 101$ kPa). Each i-th snapshot vector $\mathbf{L}$, described in Equation (3), is a flattened concatenation of the wall thickness (t_w), control point $CP3_y$, pressure distribution $\mathbf{p}_L$, temperature distribution $\mathbf{T}_L$, and Mach distribution $\mathbf{M}_L$. Since the domain was discretized using 401 cells, each snapshot has a dimension of 1025.

$$\mathbf{L} = \begin{bmatrix} t_w \\ CP3_y \\ \mathbf{p}_L \\ \mathbf{T}_L \\ \mathbf{M}_L \end{bmatrix}^{1205\times 1} \tag{3}$$

2.1.2 High fidelity model

In contrast, the high-fidelity model is a 2D Navier-Stokes solver coupled with conjugate heat transfer to the solid nozzle walls. The equations for the fluid domain were solved using the SU2 (ECONOMON et al., 2016) solver with the SST turbulence model. Additionally, the energy equation for heat transfer in the wall boundary was included. The outside wall temperature was fixed at a constant temperature ($T_w = 300$), while the inside wall temperature was calculated based on the energy balance due to heat transfer from the hot air flow to the AISI406 steel walls. In this case, the i-th snapshot takes into account the wall thickness (t_w), the third control point y-coordinate $CP3_y$, pressure field $\mathbf{p}_L$, temperature field $\mathbf{T}L$, Mach field $\mathbf{M}L$, solid temperature field $\mathbf{Ts}$, inside wall temperature distribution $\mathbf{Tiw}$, and inside wall heat flux distribution $\mathbf{q}$. As the 2D solutions are much higher dimensional, each snapshot has a 252842 dimension.

$$\mathbf{L} = \begin{bmatrix} t_w \\ CP3_y \\ \mathbf{p}_H \\ \mathbf{T}_H \\ \mathbf{T_s} \\ \mathbf{M}_H \end{bmatrix}^{252842\times 1} \tag{4}$$

2.2 Step 2: Order Reduction using SVD

The Singular Value Decomposition (SVD) is a matrix factorization method, given by Equation (5), that decomposes a matrix $\mathbf{A}$ into the product of three matrices: $\mathbf{U}$, $\mathbf{\Sigma}$, and $\mathbf{V}^T$, (WILLIAM H. PRESS et al., 2007; GOLUB; VAN LOAN, 2013).

$$\mathbf{A} = \mathbf{U}\mathbf{V}^T \tag{5}$$

Using SVD, we can approximate $\mathbf{A}$ by truncating the matrices $\mathbf{U}$, $\mathbf{\Sigma}$, and $\mathbf{V}^T$ to their first k columns, where k is a positive integer less than or equal to the

rank r of $\mathbf{A}$. This truncated SVD can be written as:

$$\mathbf{A} \approx \tilde{\mathbf{U}}\tilde{\mathbf{\Lambda}} \tag{6}$$

The cumulative summation provided by Equation (7) gives the percentage of accumulated energy preserved up to the k-th mode of SVD truncation, making it useful for assessing the quality of reconstruction using a given k modes. Figure 4 shows this metric for both the low-fidelity and high-fidelity datasets after the SVD procedure.

$$\%\ Energy_i = \sum_{j=1}^{i} \frac{\Sigma_k^2}{\sum_{l=1}^{r} \Sigma_l^2} \times 100 \quad , i = 1, 2, \ldots, r \tag{7}$$

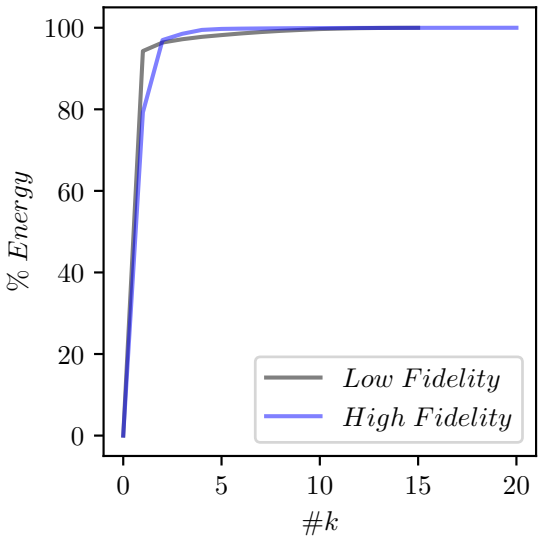

Figure 4: Percentual cumulative error of SVD reconstruction as a function of number of modes k.

The low fidelity truncated SVD used 5 modes, while the high fidelity truncated SVD used 10 modes.

2.3 Step 3: Training the Neural Network

The neural network described in this study employs the backpropagation algorithm and Mean Squared Error (MSE) as the loss function for training. The training data consists of pairs of projected matrices of basis coefficients for both low and high fidelity models ($\tilde{\mathbf{\Lambda}}_\mathbf{L}$ and $\tilde{\mathbf{\Lambda}}_\mathbf{H}$ respectively), which are obtained using Equation (9). The optimizer used is stochastic gradient descent with adaptive moment estimation (Adam), and the activation function is hyperbolic tangent. The neural network has an input and output layer with neuron counts that match the dimensions of each snapshot of basis coefficients. Additionally, there are 10 hidden layers, each with 10 neurons. The architecture of the neural network is depicted in Figure 5.

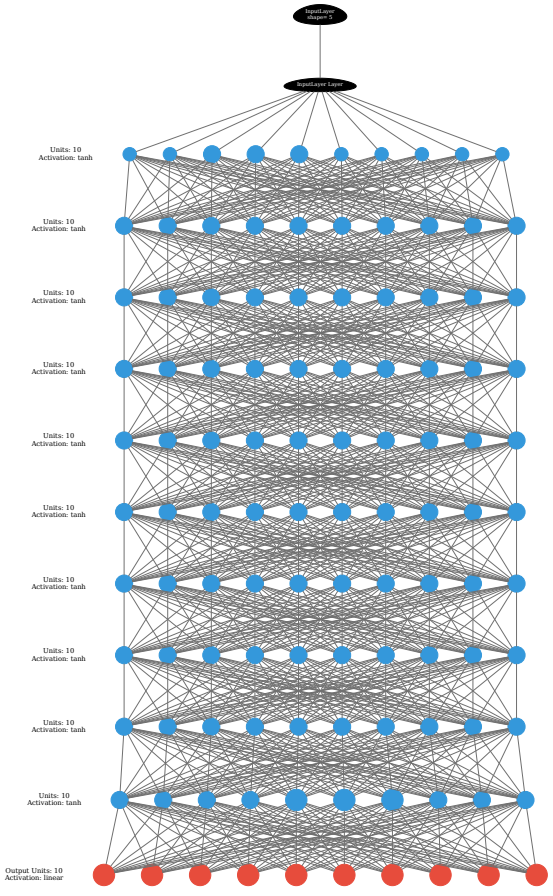

Figure 5: Neural Network architecture.

$$\tilde{\mathbf{\Lambda}}_L = \tilde{\mathbf{U}}_L^T \mathbf{A}_L \tag{8}$$

$$\tilde{\mathbf{\Lambda}}_H = \tilde{\mathbf{U}}_H^T \mathbf{A}_L \tag{9}$$

To ensure the robustness and generalization capability of the neural network, only 80 % of the available snapshots were used for the training process, while the remaining 20% was split into separate validation and test datasets. Due to the limited size of the dataset, the model was trained for a relatively short period of 300 epochs, with a training time of approximately 15 seconds.

3 Results

The proposed methodology for flow reconstruction of the internal flow and heat transfer on a rocket nozzle using neural network and singular value decomposition was evaluated by comparing the reconstructed results with the CFD simulation results. The performance of the proposed methodology was assessed using two metrics: the mean absolute error (MAE) and the coefficient of determination (R^2). The MAE measures the average magnitude of the errors between the reconstructed and CFD simulation results, while R^2 measures the proportion of the variance in the predictions. The MAE and R^2 were calculated for both fluid and solid flow fields, and the results are presented in Table 2.

	MAE	$\mathbf{R^2}$
$\mathbf{p}$	698.4111 Pa	0.9999
$\mathbf{T}$	2.7631 K	0.9958
$\mathbf{M}$	0.0026	0.9999
$\mathbf{T}_{\text{SOLID}}$	8.3579 K	0.7179
$\mathbf{T}_{\text{WALL}}$	16.757 K	0.2241
$\mathbf{q}_{\text{WALL}}$	25386.4482 W/m^2	0.8093

Table 2: Mean absolute error and coefficient of determination for surrogate model predictions.

The results demonstrate the high accuracy of the proposed methodology in reconstructing the pressure, temperature, and Mach fields, as evidenced by the high R^2 values and low MAE values. The R^2 values approach 1, indicating that the reconstructed results account for a large portion of the variance in the CFD simulation results. Additionally, the relatively small MAE values indicate that the errors between the reconstructed results and the CFD simulation results are minimal.

The pressure flow field obtained from the CFD simulation, the proposed surrogate model, and their corresponding absolute errors are presented in Figures 6, 7, and 8, respectively. The temperature flow field obtained from the CFD simulation, the proposed surrogate model, and their corresponding absolute errors are presented in Figures 9, 10, and 11, respectively. Finally, the Mach flow field obtained from the CFD simulation, the proposed surrogate model, and their corresponding absolute errors are presented in Figures 12, 13, and 14, respectively.

The proposed methodology exhibits significant potential for accurately reconstructing fluid flow and heat transfer fields in a rocket nozzle. The results indicate that the methodology can accurately reconstruct fluid flow fields, particularly the pressure field, as demonstrated in Figures 15,16 and 17. However, the surrogate model's performance was inadequate for variables in the solid domain, such as temperature and heat flux, as evident in Figure 18,19 and 20.

Combining the neural network approach with singular value decomposition results in an efficient and accurate method for reconstructing flow and heat transfer fields from low fidelity simulations. This methodology is a promising tool for designing and optimizing rocket nozzles, where accurate predictions of the flow and heat transfer fields are critical for ensuring optimal performance and safety.

Although the model's performance may be poor in some cases, it still has value. This is because the low-fidelity model alone was unable to provide a solution for the coupled heat transfer problem, and even inaccurate predictions can guide decision-making in a design process, as shown in Figures 21 and 22. While the heat transfer and wall temperature are not well predicted, the overall trend is captured.

Despite the inaccuracies in the solid field solutions, it is important to emphasize the significant speedup achieved by the surrogate model. While high-fidelity CFD took about 1 hour and 30 minutes to complete, the surrogate model can predict a flow field within just 10.6 seconds (an astonishing 500-fold speedup). It's important to note that this time includes the time needed to generate the mesh for a new geometry, as during data projection into the latent space, all spatial information is lost.

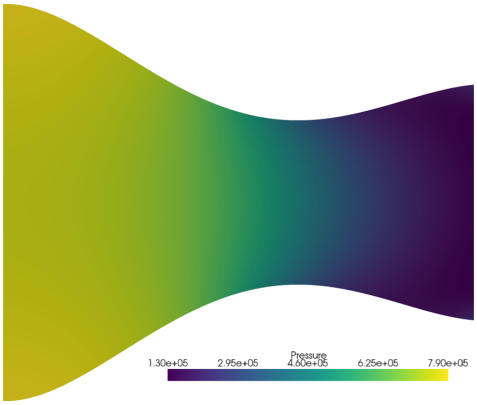

Figure 6: CFD pressure $[Pa]$ flow field.

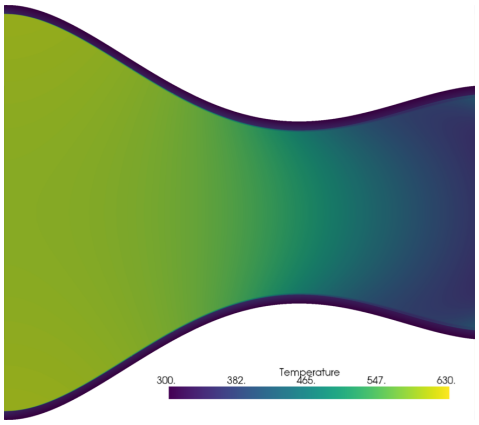

Figure 9: CFD temperature $[K]$ flow field.

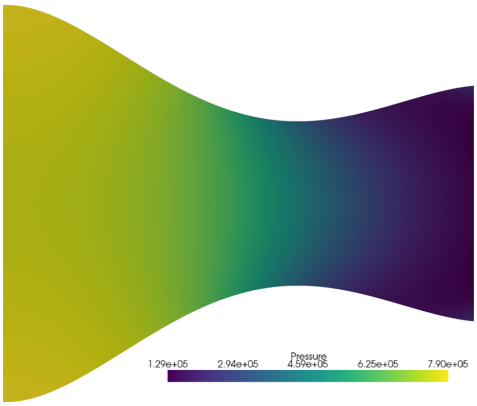

Figure 7: Surrogate model prediction of pressure $[Pa]$ flow field.

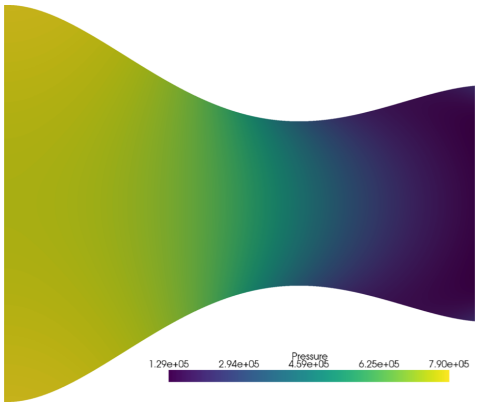

Figure 10: Surrogate model prediction of temperature $[K]$ flow field.

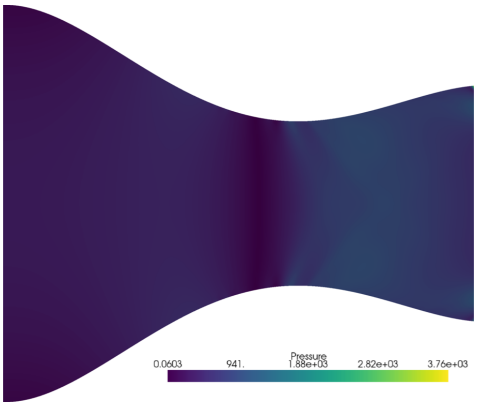

Figure 8: Absolute error of surrogate model prediction of pressure $[Pa]$ flow field.

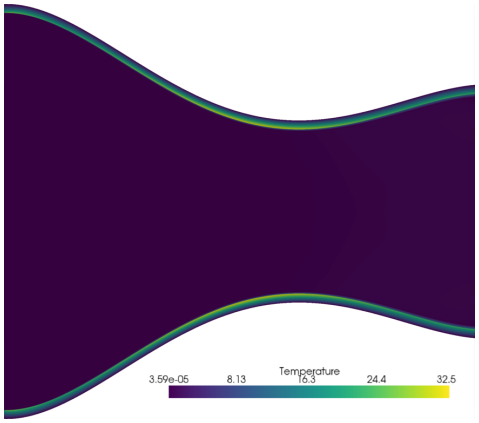

Figure 11: Absolute error of surrogate model prediction of temperature $[K]$ flow field.

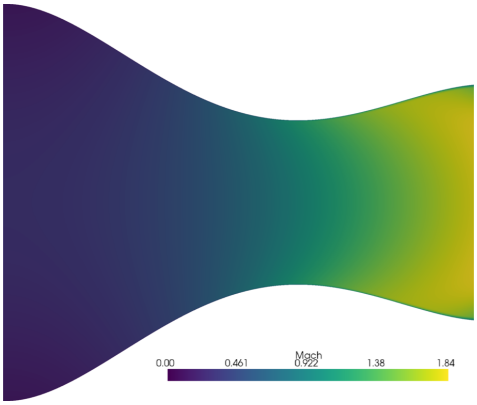

Figure 12: CFD Mach flow field.

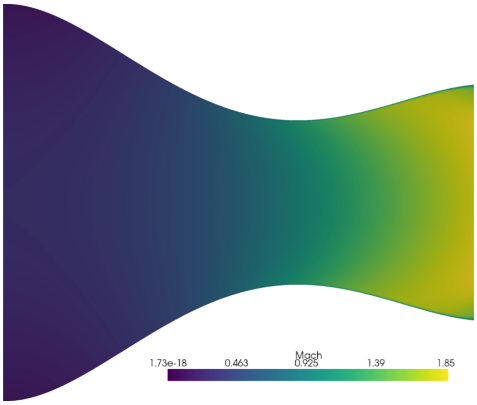

Figure 13: Surrogate model prediction of Mach flow field.

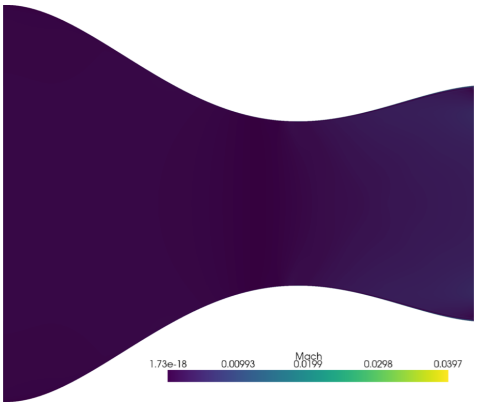

Figure 14: Absolute error of surrogate model prediction of Mach flow field.

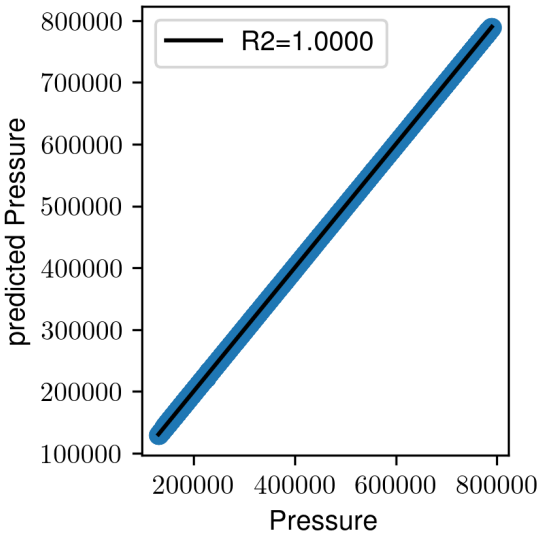

Figure 15: Surrogate model prediction of pressure $[Pa]$ flow fields over test dataset.

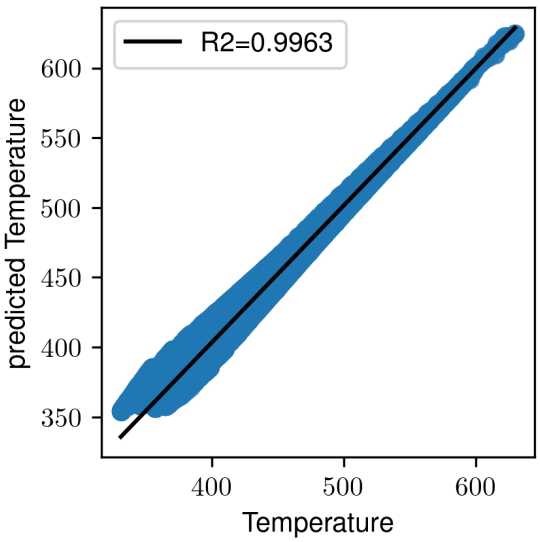

Figure 16: Surrogate model prediction of temperature $[K]$ flow fields over test dataset.

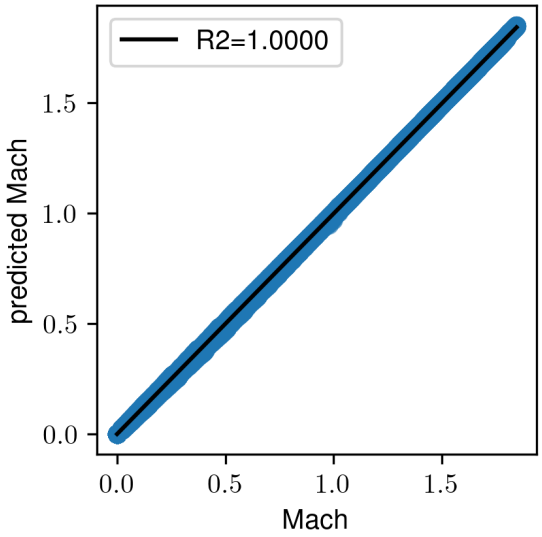

Figure 17: Surrogate model prediction of Mach flow fields over test dataset.

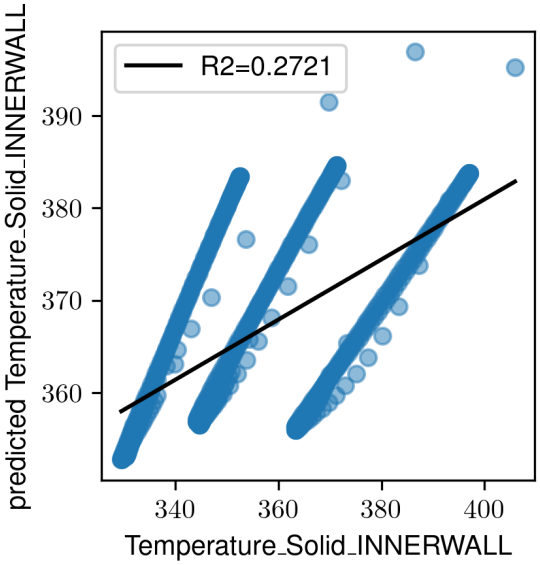

Figure 19: Surrogate model prediction of nozzle wall surface temperature $[K]$ distributions over test dataset.

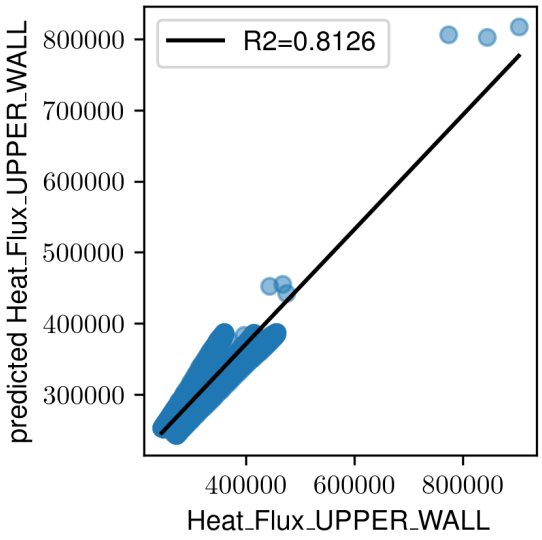

Figure 18: Surrogate model prediction of heat flux $[W/m^2]$ distributions over test dataset.

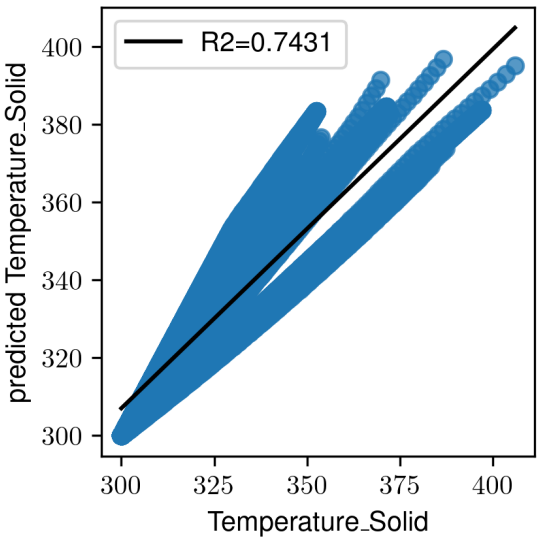

Figure 20: Surrogate model prediction of nozze wall temperature $[K]$ field over test dataset.

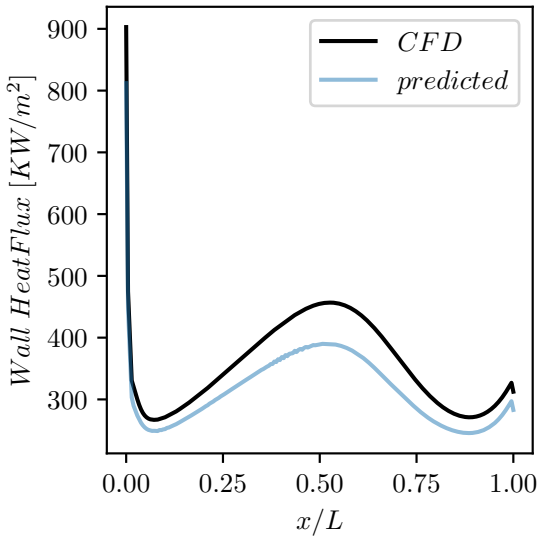

Figure 21: Surrogate model prediction of a heat flux $[W/m^2]$ distribution.

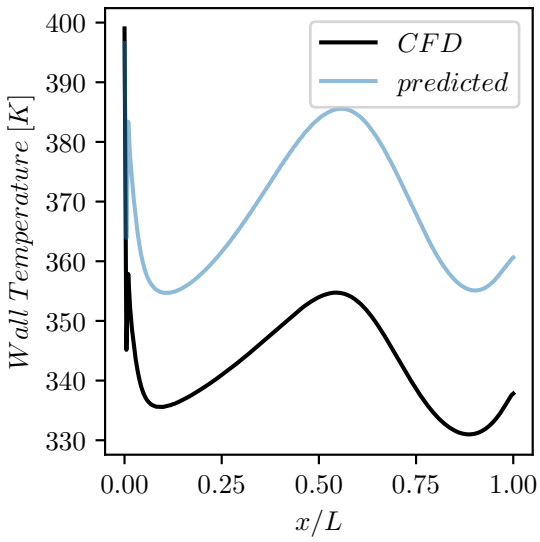

Figure 22: Surrogate model prediction of a nozzle wall surface temperature $[K]$ distribution.

3.1 Model Limitations and Improvements Suggestions

However, one major drawback of the model is the need for a large amount of data for training. Since the dataset used for training is quite small, adding more snapshots is expected to improve model accuracy. Additionally, using more elaborate individual normalization techniques for each variable could help the model. Another suggestion is to perform hyperparameter optimization on the number of layers and neurons, activation functions, and try more advanced loss functions and optimization algorithms. Moreover, redesigning the variables selected to compose the dataset could also help improve the model. Replacing single scalar values of wall thickness and the y-coordinate of the control point with a distribution of wall thickness and the distribution of y-coordinates for the nozzle wall could help the model to predict variability associated with the wall contour change.

4 Conclusion and Future Work

In conclusion, although our methodology did not introduce any novel techniques, it proved to be effective in accurately reconstructing the fluid flow in a rocket nozzle using neural network and singular value decomposition. However, we acknowledged that the methodology's performance was limited in reconstructing the heat flux and wall temperature fields. We provided suggestions for improving the methodology and suggested increasing the sample size in the dataset and comparing our model with other surrogate models as future work. Despite these limitations, the proposed methodology has the potential to enhance the design and optimization cycle by offering a more precise understanding of flow and heat transfer while reducing computational cost.

A Code Repository

The code utilized and developed for this project can be found in its entirety on the corresponding GitHub repository (CARVALHO, 2023).

Bibliography

BRUNTON, S. L.; KUTZ, J. N. *Data-driven science and engineering*. Cambridge, England: Cambridge University Press, February 2019.

CARVALHO, A. M. *A Flow Reconstruction Framework written in python*. [S.l.: s.n.], April 2023. Available from: ¡https : / / github . com / properallan/ihtc_repository¿.

ECONOMON, T. D. et al. SU2: An Open-Source Suite for Multiphysics Simulation and Design. *AIAA Journal*, American Institute of Aeronautics and Astronautics (AIAA), v. 54, n. 3, p. 828–846, March 2016. DOI: 10.2514/1.j053813. Available from: ¡https://doi.org/10.2514/1.j053813¿.

GOLUB, G. H.; VAN LOAN, C. F. *Matrix Computations*. 4. ed. Baltimore, MD: Johns Hopkins University Press, February 2013. (Johns Hopkins Studies in the Mathematical Sciences).

HIRSCH, C. *Numerical computation of internal and external flows: The fundamentals of computational fluid dynamics*. 2. ed. Oxford, England: Butterworth-Heinemann, June 2007.

LUI, H. F. S.; WOLF, W. R. Construction of reduced-order models for fluid flows using deep feedforward neural networks. *Journal of Fluid Mechanics*, Cambridge University Press (CUP), v. 872, p. 963–994, June 2019. DOI: 10.1017/jfm.2019.358. Available from: ¡https://doi.org/10.1017/jfm.2019.358¿.

MCKAY, M. D.; BECKMAN, R. J.; CONOVER, W. J. A Comparison of Three Methods for Selecting Values of Input Variables in the Analysis of Output from a Computer Code. *Technometrics*, JSTOR, v. 21, n. 2, p. 239, May 1979. DOI: 10.2307/1268522. Available from: ¡https://doi.org/10.2307/1268522¿.

WILLIAM H. PRESS et al. *Numerical recipes 3rd edition*. 3. ed. Cambridge, England: Cambridge University Press, September 2007.

YU, J.; HESTHAVEN, J. S. Flowfield Reconstruction Method Using Artificial Neural Network. *AIAA Journal*, American Institute of Aeronautics and Astronautics (AIAA), v. 57, n. 2, p. 482–498, February 2019. DOI: 10.2514/1.j057108. Available from: ¡https : / / doi . org / 10 . 2514 / 1 . j057108¿.

ZHANG, X. Coupled simulation of heat transfer and temperature of the composite rocket nozzle wall. *Aerospace Science and Technology*, Elsevier BV, v. 15, n. 5, p. 402–408, July 2011. DOI: 10.1016/j.ast.2010.09.006. Available from: ¡https://doi.org/10.1016/j.ast.2010.09.006¿.